Probing neutrino nature and time reversal symmetry violation in elastic scattering of low energy neutrinos on polarized electrons in presence of non-standard couplings

{ Wiesław Sobków and Arkadiusz Błaut}@uwr.edu.pl
Institute of Theoretical Physics, University of Wrocław, Poland

Introduction

- no difference between Dirac and Majorana neutrinos (νs) in standard model (SM) [1] with V-A interaction (**left-handed chirality** (LC) of νs) in relativistic ν limit
- no time reversal symmetry violation (TRSV) in leptonic processes, e.g. neutrino-electron elastic scattering (NEES)
- single CP violating phase of CKM quark mixing matrix does not explain matter-antimatter asymmetry of universe (**new TRSV phases are required**)
- origin of parity violation is not clarified
- background problem in low energy ν experiments
- experimental results still leave space for non-standard complex S, T, P couplings of **right chiral** (RC) νs
- polarized electron target (PET) as new tool sensitive to interferences between V-A and S, T, P interactions
- PET may be helpful in detecting TRSV and shed some light on ν nature, and other open questions: precise measurement of background level in low energy solar νs, ν magnetic moments, the flavour composition of $(\overline{\nu})\nu$ beam, axions, spin-spin interaction in gravitation [2-8]

Assumptions

- detection process is elastic scattering of low energy ν_es on **polarized electrons** of target (ESNPE): $\nu_e + e^- \to \nu_e + e^-$
- amplitude for Dirac νs:

$$M^D_{\nu_e e^-} = \frac{G_F}{\sqrt{2}}\{(\overline{u}_{e'}\gamma^\alpha(c_V^L - c_A^L\gamma_5)u_e)(\overline{u}_{\nu_{e'}}\gamma_\alpha(1-\gamma_5)u_{\nu_e}) + c_S^R(\overline{u}_{e'}u_e)(\overline{u}_{\nu_{e'}}(1+\gamma_5)u_{\nu_e}) + c_S^L(\overline{u}_{e'}u_e)(\overline{u}_{\nu_{e'}}(1-\gamma_5)u_{\nu_e}) + \text{other interactions } c_V^R,\ c_A^R,\ c_P^{R,L},\ c_T^{R,L}\} \quad (1)$$

- coupling constants are denoted respectively to the incoming ν_e of left- (L) and right-handed (R) chirality
- $c_S^{R,L}$, $c_P^{R,L}$, $c_T^{R,L}$ are complex numbers and $c^L_{S,T,P} = c^{*R}_{S,T,P}$
- amplitude for Majorana ν_es does not contain vector V and tensor T interactions in ν_e current
- incoming ν_e beam comes from (un)polarized source and is linear superposition of LC with RC states
- transversal components of ν_e spin polarization (TCNSP) as consequence of left-right superposition
- model-independent considerations for flavour-conserving interactions in limit of vanishing ν_e mass.

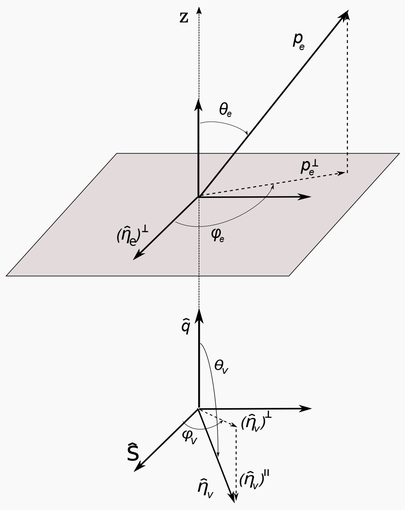

Fig. 1. Production plane of ν_e beam is spanned by polarization unit vector $\hat{\boldsymbol{S}}$ of source and ν_e LAB momentum unit vector $\hat{\mathbf{q}}$. Reaction plane is spanned by $\hat{\mathbf{q}}$ and transverse electron polarization vector of target $(\hat{\boldsymbol{\eta}}_{\boldsymbol{e}})^\perp$ (due to $\hat{\boldsymbol{\eta}}_{\boldsymbol{e}} \perp \hat{\mathbf{q}}$). θ_e is polar angle between $\hat{\mathbf{q}}$ and the unit vector $\hat{\mathbf{p}}_e$ of recoil electron momentum. ϕ_e is the angle between $(\hat{\boldsymbol{\eta}}_{\boldsymbol{e}})^\perp$ and the transversal component of outgoing electron momentum $(\hat{\mathbf{p}}_e)^\perp$. $\hat{\boldsymbol{\eta}}_{\boldsymbol{\nu}} = (\sin\theta_\nu\ \cos\phi_\nu, \sin\theta_\nu\ \sin\phi_\nu, \cos\theta_\nu)$.

Conclusions

When incoming ν_es are only LC, but S, T interactions participate in ESNPE, then azimuthal asymmetry, Fig.4, is sensitive to TRSV and indicates Dirac νs independently of exotic couplings for Majorana νs. When ν_e beam is superposition of LC with RC states azimuthal asymmetries, Figs. 5-6, and spectrum of recoil electrons, Figs.7-8, contain interferences between $V-A$ and S, P, T couplings for Dirac νs (and between $V-A$ and only S, P for Majorana νs) related to $(\hat{\boldsymbol{\eta}}_{\boldsymbol{\nu}})^\perp$ of production process. It allows us to test TRSV, probe ν_e nature and search for RC νs. Today controlled production of ν_e beam with fixed direction of $(\hat{\boldsymbol{\eta}}_{\boldsymbol{\nu}})^\perp$ is still impossible. Tests require intense low-energy ν_e sources, PET, and detectors sensitive to azimuthal angle and polar angle of scattered electrons with good angular resolution. It is worth highlighting that feasibility of electron polarized scintillating target has been confirmed by [9]).

Results

standard V-A interaction with only LC νs

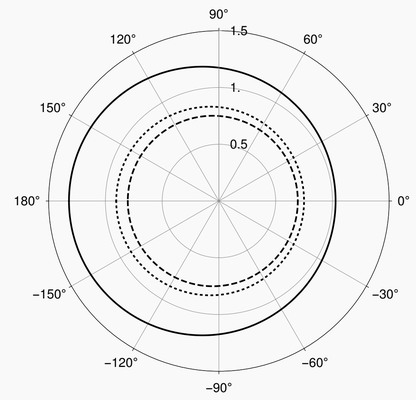

Fig. 2. Dependence of $d^2\sigma/d\phi_e d\,\theta_e$ on ϕ_e for $\hat{\boldsymbol{\eta}}_{\boldsymbol{\nu}} \cdot \hat{\mathbf{q}} = -1$, $E_\nu = 1\,MeV$: $\theta_e = \pi/12$ (dotted line), $\theta_e = \pi/6$ (solid line), $\theta_e = \pi/3$ (dashed line)

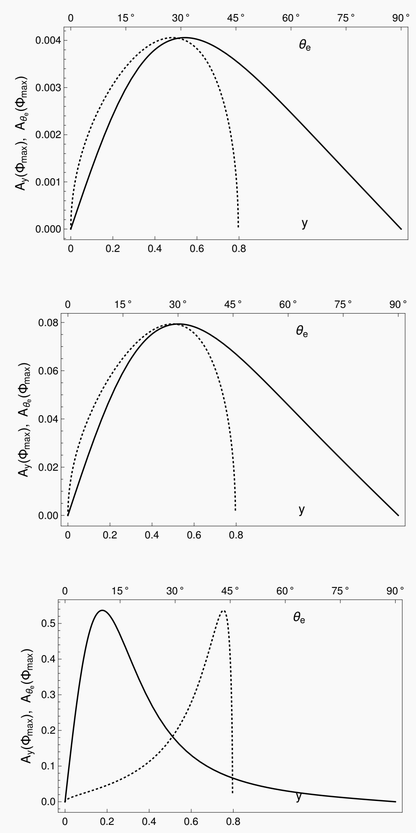

Fig.3. $A_y(\Phi) := \dfrac{\int_{\Phi}^{\Phi+\pi} \frac{d^2\sigma}{d\phi_e dy}\, d\phi_e - \int_{\Phi+\pi}^{\Phi+2\pi} \frac{d^2\sigma}{d\phi_e dy}\, d\phi_e}{\int_{\Phi}^{\Phi+\pi} \frac{d^2\sigma}{d\phi_e dy}\, d\phi_e + \int_{\Phi+\pi}^{\Phi+2\pi} \frac{d^2\sigma}{d\phi_e dy}\, d\phi_e}$.

$A_{\theta_e}(\Phi) := \dfrac{\int_{\Phi}^{\Phi+\pi} \frac{d^2\sigma}{d\phi_e d\theta_e}\, d\phi_e - \int_{\Phi+\pi}^{\Phi+2\pi} \frac{d^2\sigma}{d\phi_e d\theta_e}\, d\phi_e}{\int_{\Phi}^{\Phi+\pi} \frac{d^2\sigma}{d\phi_e d\theta_e}\, d\phi_e + \int_{\Phi+\pi}^{\Phi+2\pi} \frac{d^2\sigma}{d\phi_e d\theta_e}\, d\phi_e}$

Plot of $A_y(\Phi_{max})$ as a function y (dotted line) and $A_{\theta_e}(\Phi_{max})$ as a function of θ_e (solid line) for $\hat{\boldsymbol{\eta}}_{\boldsymbol{\nu}} \cdot \hat{\mathbf{q}} = -1$, $E_\nu = 1\,MeV$, $\Phi_{max} = \pi/2$: upper plot for $\theta_1 = 0.1$; middle plot for $\theta_1 = \pi/2$; lower plot for $\theta_1 = \pi - 0.1$.

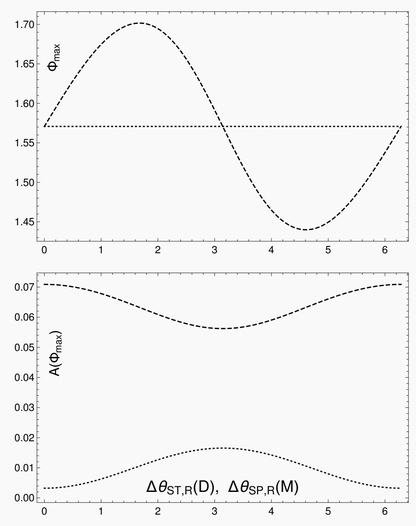

Fig. 4. $A(\Phi) := \dfrac{\int_{\Phi}^{\Phi+\pi} \frac{d\sigma}{d\phi_e}\, d\phi_e - \int_{\Phi+\pi}^{\Phi+2\pi} \frac{d\sigma}{d\phi_e}\, d\phi_e}{\int_{\Phi}^{\Phi+\pi} \frac{d\sigma}{d\phi_e}\, d\phi_e + \int_{\Phi+\pi}^{\Phi+2\pi} \frac{d\sigma}{d\phi_e}\, d\phi_e}$

Upper plot (dashed line) is the dependence of Φ_{max} on $\Delta\theta_{ST,R}(D)$ for Dirac ν_e in case of $V-A$, S_R and T_R interactions when $|c_S^R| = |c_T^R| = 0.2$. Upper plot (dotted line) is the dependence of Φ_{max} on $\Delta\theta_{SP,R}(M)$ for Majorana ν_e in case of $V-A$, S_R, P_R couplings when $|c_S^R| = |c_P^R| = 0.2$. Both scenarios for $\hat{\boldsymbol{\eta}}_{\boldsymbol{\nu}} \cdot \hat{\mathbf{q}} = -1$, $\theta_1 = \pi/2, E_\nu = 1\,MeV$. Lower plot is the dependence of $A(\Phi_{max})$ on $\Delta\theta_{ST,R}(D)$ for Dirac ν_e (dashed line) and on $\Delta\theta_{SP,R}(M)$ for Majorana ν_e (dotted line), respectively, (the same assumptions as for Φ_{max}).

References

[1] S. L. G., Nucl. Phys. **22**, 579 (1961). S. W., Phys. Rev. Lett. **19**, 1264 (1967). A. S., in *Elementary Particle Theory* (Almquist and Wiksells, Stockholm, 1969). [2] M. M. et al., Nucl. Phys. B **734**, 203 (2006). [3] S. C. et al., Phys. Rev. D **71**, 093006 (2005); **W**. Sobków, A. Błaut, Eur. Phys. J. C (2018) 78:197; arXiv:1812.09828. [4] J. B. et al., Phys. Lett. B **613**, 162 (2005). [5] V. A. G. et al., Phys. Rev. D **75**, 073021 (2007). [6] P. M., M. P., Phys. Lett. B **541**, 151 (2002). [7] T. I. R., V. B. S., Phys. Lett. B **479**, 218 (2000). [8] W. Rodejohann at al., JHEP **05**, 024 (2017). [9] B. B. et al., Nucl. Instrum. and Meth. A **694**, 335 (2012).

Recoil electrons azimuthal asymmetry

superposition LC with RC νs in presence of exotic interactions S, T, P, V+A

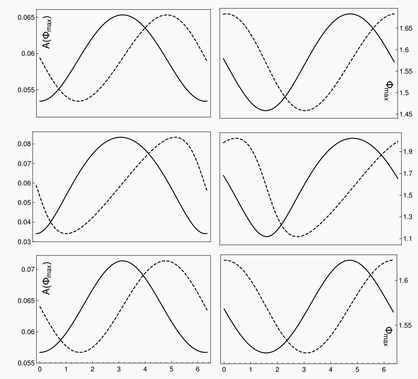

Fig. 5. Dependence of $A(\Phi_{max})$ on ϕ_ν (solid line) and Φ_{max} on ϕ_ν (dashed line) for $E_\nu = 1\,MeV, \theta_1 = \pi/2$. TRSC: upper left plot for Dirac ν ($V-A$ with S_R, $|c_S^R| = 0.2, \theta_{S,R} = 0$); middle left plot for Majorana ν (the same couplings as for Dirac ν); lower left plot for Dirac ν ($V-A$ with T_R, $|c_T^R| = 0.2, \theta_{T,R} = 0$). TRSV: upper right plot for Dirac ν; middle right plot for Majorana case; lower right plot for Dirac case (exactly the same assumptions as for TRSC, but now $\theta_{S,R} = \pi/2, \theta_{T,R} = \pi/2$).

Azimuthal asymmmetry $A_{\theta_e}(\Phi_{max})$

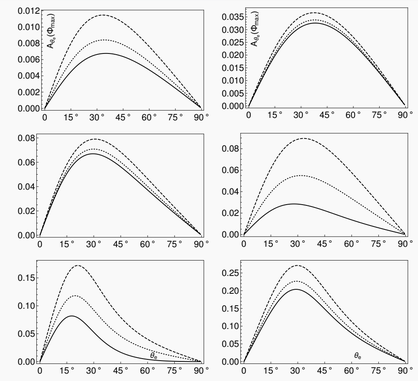

Fig. 6. $A_{\theta_e}(\Phi_{max})$ as a function of θ_e for the case of $V-A$ with S_R ($E_\nu = 1\,MeV$, $\phi_\nu = 0$, $\hat{\boldsymbol{\eta}}_{\boldsymbol{\nu}} \cdot \hat{\mathbf{q}} = -0.95$);left column for Dirac ν, right column for Majorana ν; upper plot for $\theta_1 = 0.1$; middle plot for $\theta_1 = \pi/2$; lower plot for $\theta_1 = \pi - 0.1$; solid line for $|c_S^R| = 0.3$, $\theta_{S,R} = 0$; dotted line for $|c_S^R| = 0.3$, $\theta_{S,R} = \pi/4$; dashed line for $|c_S^R| = 0.3$, $\theta_{S,R} = \pi/2$.

Spectrum of recoil electrons

Fig. 7. Dependence of $d\sigma/dy$ on y for $\hat{\boldsymbol{\eta}}_{\boldsymbol{\nu}} \cdot \hat{\mathbf{q}} = -0.95, E_\nu = 1\,MeV$, $\phi_\nu = 0$. Upper plot for TRSC: standard $V-A$ interaction (solid line); Dirac ν for $V-A$ with T_R, $|c_T^R| = 0.3, \theta_{T,R} = 0$ (dashed-dotted line) and for $V-A$ with S_R $|c_S^R| = 0.3, \theta_{S,R} = 0$ (dotted line); Majorana ν for $V-A$ with S_R, $|c_S^R| = 0.3, \theta_{S,R} = 0$ (dashed line). Lower plot for TRSV: $V-A$ interaction (solid line); $V-A$ with T_R (dashed-dotted line); $V-A$ with S_R (dotted line); Majorana ν for $V-A$ with S_R (dashed line) (exactly the same assumptions as for TRSC, but now $\theta_{S,R} = \pi/2, \theta_{T,R} = \pi/2$).

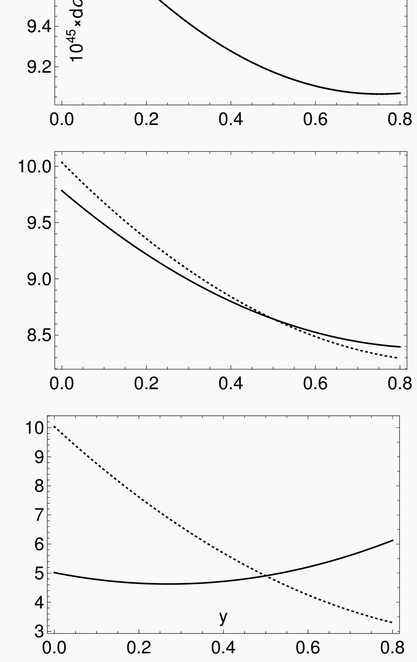

Fig. 8. $d\sigma/dy$ as a function of y for $V-A$ with S_R, $c_S^R = 0.3$, $\theta_1 = \pi/2$; $\hat{\boldsymbol{\eta}}_{\boldsymbol{\nu}} \cdot \hat{\mathbf{q}} = -1$ (upper plot), $\hat{\boldsymbol{\eta}}_{\boldsymbol{\nu}} \cdot \hat{\mathbf{q}} = -0.95$ (middle plot), $\hat{\boldsymbol{\eta}}_{\boldsymbol{\nu}} \cdot \hat{\mathbf{q}} = 0$ (lower plot), for Dirac (solid line) and Majorana (dotted line) ν_es.